

# Investigation of conductivity of adhesive layer including indium tin oxide particles for multi-junction solar cells

Shinya Yoshidomi · Masahiko Hasumi ·  
Toshiyuki Sameshima

Received: 26 December 2013 / Accepted: 28 March 2014  
© Springer-Verlag Berlin Heidelberg 2014

**Abstract** We report connection conductivity ( $C_c$ ) of adhesive which including  $\text{In}_2\text{O}_3\text{-SnO}_2$  (ITO) particles developed for fabrication of stacked-type-multi-junction solar cells. The commercial 20- $\mu\text{m}$  sized ITO particles were heated in vacuum at temperature ranging from 800 to 1,300 °C for 10 min to increase  $C_c$ . 6.2 wt% ITO particles were dispersed in commercial Cemedine adhesive gel to form 100 samples structured with n-type Si/adhesive/n-type Si (n-Si sample) and p-type Si/adhesive/p-type Si (p-Si sample). Current density as a function of voltage (J–V) characteristics gave  $C_c$ . It ranged from 4.3 to 1.0  $\text{S}/\text{cm}^2$  for the n-Si sample with 800 °C heat-treated ITO particles. Its standard deviation was 0.59  $\text{S}/\text{cm}^2$ . On the other hand, it ranged from 2.0 to 0.6  $\text{S}/\text{cm}^2$  for the p-Si sample with 800 °C heat-treated ITO particles. Its standard deviation was 0.22  $\text{S}/\text{cm}^2$ . The distribution of  $C_c$  mainly resulted from contact efficiency of ITO particles to substrate. We theoretically estimated that present  $C_c$  achieved a low loss of the power conversion efficiency ( $E_{\text{ff}}$ ) lower than 0.3 % in the application of fabrication of multi-junction solar cell with an intrinsic  $E_{\text{ff}}$  of 30 % and an open circuit voltage above 1.9 V.

**Keywords** Multi-junction solar cell · Indium tin oxide · X-ray diffraction · Transparent conductive layer

## 1 Introduction

Semiconductor solar cells have been investigated as a clean device which converts sunlight into electrical power [1–5].

---

S. Yoshidomi · M. Hasumi · T. Sameshima (✉)  
Tokyo University of Agriculture and Technology,  
2-24-16 Naka-cho, Koganei, Tokyo 184-8588, Japan  
e-mail: tsamesim@cc.tuat.ac.jp

Multi-junction solar cells are attractive for effectively collecting sunlight, which has a wide range spectrum from ultra violet to infrared. Technique for fabrication of multi-junction solar cell by epitaxial growth has been investigated [6–17]. However, mass production requires fabrication of large-size solar cells at low cost [18]. We proposed fabrication of multi-junction solar cells by stacking individual solar cells used by intermediate adhesive layers [19]. Intermediate adhesive layer including  $\text{In}_2\text{O}_3\text{-SnO}_2$  (ITO) particles which is conductive and transparent has been reported [19–21]. Moreover, the stacking of fragile 4-inch-sized GaAs and Ge substrates has been reported [22]. We reported intermediate adhesive layer including ITO with connection conductivity ( $C_c$ ) of 0.56  $\text{S}/\text{cm}^2$  [22]. Our reports indicated possibility for fabrication of multi-junction solar cells by stacking fragile and large size materials. However, improvement of conductivity of intermediate layer and control of distribution of conductivity are still required. In this paper, we discuss required conductivity for multi-junction solar cells. We report change in ITO particles by heating in vacuum using X-ray diffraction measurement. Then, we report distribution of  $C_c$  of intermediate layer.

## 2 Theoretical estimation of connection conductivity for multi junction solar cells

We theoretically estimated changes in solar cell characteristics and their conversion efficiencies with connection conductivity. The effective characteristic of multi-junction solar cells was assumed to be given by the theoretical formula with one PN diode and a series resistivity  $R_s$  giving a reciprocal  $C_c$  [23–26].

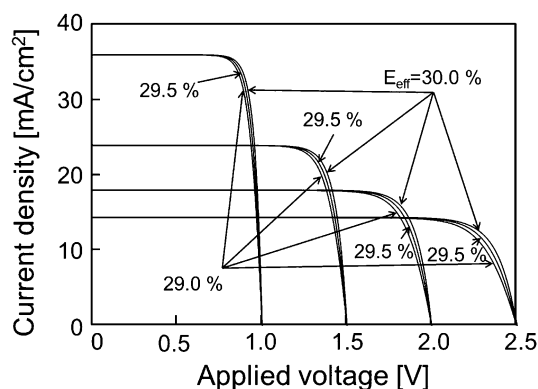


**Fig. 1** Calculated solar cell characteristics with the effective conversion efficiency  $E_{\text{ff}}$  of 29.0, 29.5 and 30 % with different  $V_{\text{oc}}$

$$J = J_0 \left\{ \exp \left( \frac{q(V - R_s J)}{nkT} \right) - 1 \right\} + \frac{V - R_s J}{R_{\text{sh}}} - J_{\text{ph}} \quad (1)$$

$$= J_0 \left\{ \exp \left( \frac{q \left( V - \frac{J}{C_c} \right)}{nkT} \right) - 1 \right\} + \frac{V - \frac{J}{C_c}}{R_{\text{sh}}} - J_{\text{ph}}$$

where  $J$ ,  $J_0$ ,  $R_{\text{sh}}$ ,  $n$ , and  $J_{\text{ph}}$  are current density, saturation current density, parallel resistivity, ideality factor, and photo current density, respectively. Intrinsic conversion efficiency ( $E_{\text{ff}}$ ), i.e., in the case of  $C_c$  becomes large enough, of 30 % was set to discuss the  $C_c$  in the equivalent circuit given above. Self-consistent calculation was conducted with different open circuit voltages ( $V_{\text{oc}}$ ) in the range from 1.0 to 2.5 V for practical multi-junction solar cells.  $C_c$  limits the electrical current density in the circuit and changes solar cell characteristics. Therefore,  $C_c$  decreases effective  $E_{\text{ff}}$  in general. In the condition of the same effective  $E_{\text{ff}}$ , a high  $V_{\text{oc}}$  allows a low  $J_{\text{sc}}$  and low  $C_c$ . Figure 1 shows calculated solar cell characteristics with the effective  $E_{\text{ff}}$  of 29.0, 29.5 and 30.0 %. In the case of solar cell characteristics with  $V_{\text{oc}}$  of 1.0 V,  $C_c$  of 2.35 and 1.18 S/cm<sup>2</sup> were allowed to achieve  $E_{\text{ff}}$  of 29.5 and 29.0 %, respectively. On the other hand, in the case of  $V_{\text{oc}}$  of 2.5 V,  $C_c$  of 0.38 and 0.19 S/cm<sup>2</sup> were allowed to achieve effective  $E_{\text{ff}}$  of 29.5 and 29.0 %, respectively. Solar cell characteristics with low  $V_{\text{oc}}$  are strongly affected by  $C_c$ . On the other hand, in the case of solar cell with high  $V_{\text{oc}}$ , low  $C_c$  is allowed. Figure 2 shows the  $C_c$  as a function of  $V_{\text{oc}}$  with effective  $E_{\text{ff}}$  of 28.0, 29.0, 29.5, and 29.7 % obtained from the J–V characteristics calculation shown in Fig. 1.  $C_c$  decreased as  $V_{\text{oc}}$  increased with every effective  $E_{\text{ff}}$  case.  $C_c$  at least 1.1 S/cm<sup>2</sup> is necessary for achieving the effective  $E_{\text{ff}}$  above 29.0 %, which meant an efficient loss of 1.0 %, for  $V_{\text{oc}}$  at 1.0 V because high electrical current needs with low  $V_{\text{oc}}$ . On the other hand,  $C_c$  of 1.1 S/cm<sup>2</sup> achieved the effective  $E_{\text{ff}}$  higher than 29.5 % for  $V_{\text{oc}}$  above 1.5 V because low photo-induced current was

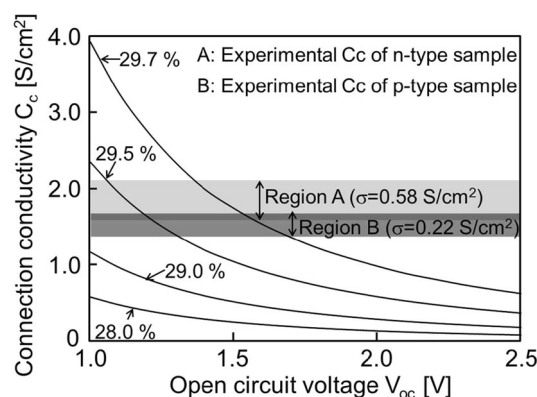


**Fig. 2**  $C_c$  as a function of  $V_{\text{oc}}$ . The curves show  $C_c$  as a function of  $V_{\text{oc}}$  with effective  $E_{\text{ff}}$  of 28.0, 29.0, 29.5 and 29.7 %. Region A and B represent experimental  $C_c$  within standard deviation of one  $\sigma$  of n-type and p-type sample, respectively

allowed. Multi-junction solar cells with high  $V_{\text{oc}}$  have, therefore, an advantage of low connection conductivity (high connection resistivity) in the fabrication of the solar cells. In this paper, we aimed to establish  $C_c$  above 1.1 S/cm<sup>2</sup> for fabricating solar cells with an effective  $E_{\text{ff}}$  above 29.5 % associated with  $V_{\text{oc}}$  above 1.5 V.

### 3 Experimental

ITO particles were made by Kojundo Chemical Laboratory Co., Ltd.: light green particles were formed by heat treatment of 95 wt%-In<sub>2</sub>O<sub>3</sub> and 5 wt%-SnO<sub>2</sub> powders in air atmosphere. Then, we selected 20  $\mu\text{m}$ -sized particles by mechanical filtering with metal mesh membranes in our laboratory. Then, the ITO particles of 350 mg were placed in a central hollow of Ta boards with a size of 2.0  $\times$  0.9 cm<sup>2</sup>. They were set in a vacuum chamber. The chamber was evacuated to 4.0  $\times$  10<sup>-4</sup> Pa. The Ta boards were heated by applying electrical power from 40 to 60 W for 10 min. Light emission from the heated Ta boards indicated that they were heated from 800 to 1,300 °C. Magnetic quadrupole mass spectrometry measurement revealed that oxygen partial pressure increased from 1.47  $\times$  10<sup>-5</sup> to 3.5  $\times$  10<sup>-5</sup> Pa as heating temperature increased from 800 to 1,300 °C. X-ray diffraction (XRD) measurement was performed with X-ray diffractometer (SmartLab, Rigaku corporation) using CuK $\alpha$  with a Ni filter for cutting CuK $\beta$ . Crystalline states and composition ratio were precisely analyzed from experimental XRD data with Rietveld refinement using software of PDXL (Rigaku corporation). Then, ITO particles were dispersed in Cemedine, which was a commercial transparent epoxy-type adhesive. Base resin and hardener gels of Cemedine and ITO particles at 6.2 wt% were mixed together and they

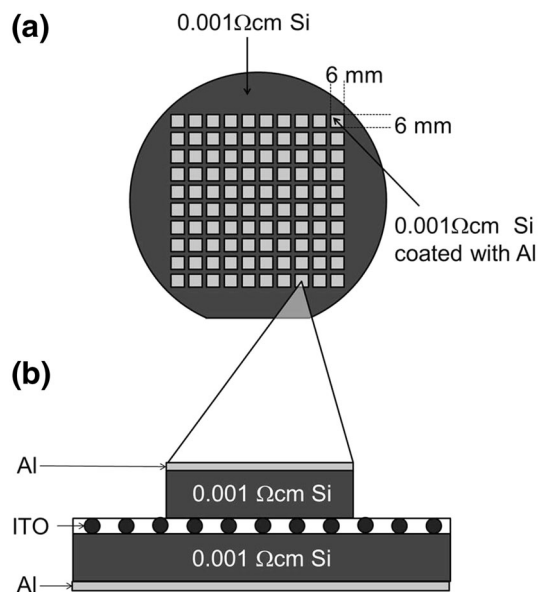


**Fig. 3** Schematic structure of sample. The overview of sample (a) and the cross section of sample (b)

were coated over the surfaces of 4-inch n- or p-type 0.001  $\Omega$  cm Si substrates. Their rear surfaces were coated with Al layers formed with the metal evaporation method for  $C_c$  measurement. 100 n or p-type 0.001  $\Omega$  cm Si pieces with a size of  $0.6 \times 0.6$  cm<sup>2</sup> with rear surface coated with Al layers were also prepared. They were then placed on the adhesive to form structure of Si/ITO/Si, as shown in Fig. 3. The Cemedine intermediate layers including ITO particles were hardened under a pressure at  $4 \times 10^5$  Pa for 1 h. 100 n-type Si pieces/ITO + Cemedine/n-type Si substrate (n-type Si sample) and 100 p-type Si pieces/ITO + Cemedine/p-type Si substrate (p-type Si sample) were consequently fabricated. 100 J–V characteristics were measured for applying voltage to every Si piece each.  $C_c$  was obtained by average value of J/V at +0.1 and –0.1 V each piece.

#### 4 Results and discussion

The weight of ITO particles were decreased from 350 mg to 300, 270, and 205 mg after the heat treatment in  $4.0 \times 10^{-4}$  Pa at 800, 1,000, and 1,300 °C for 10 min, respectively. Detailed structural change of ITO particles by the heat treatment was investigated by the XRD measurement. Figure 4 shows arbitrary diffracted intensity of XRD measurement for the initial and heat-treated ITO particles. All peaks observed in Fig. 4 were assigned to  $\text{In}_2\text{O}_3$  or  $\text{SnO}_2$ . No impurity peaks was observed. The details of peaks from a to g in Fig. 4 are described in Table 1. The peaks of b and e, assigned to  $\text{SnO}_2$ , abated as the heating temperature increased. Especially, in the case of 1,300 °C

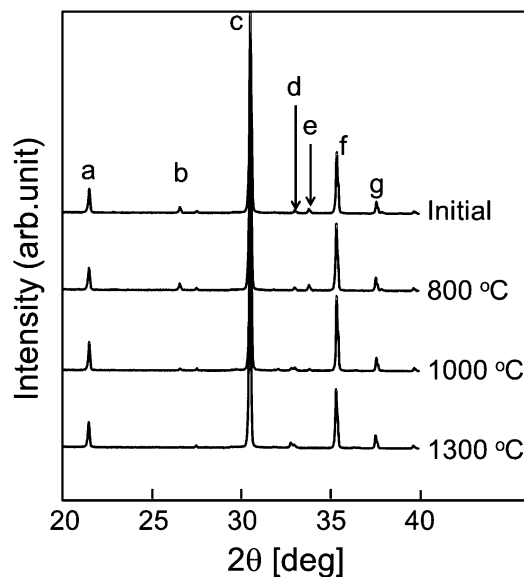


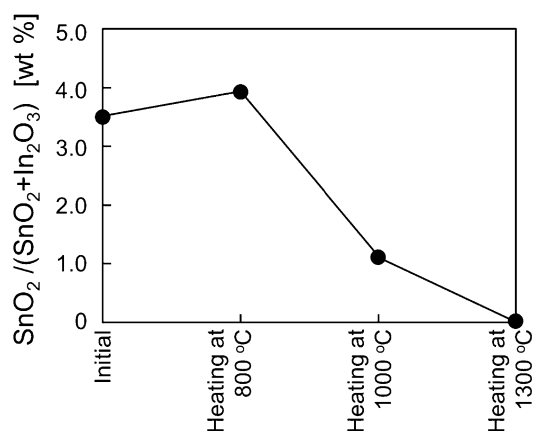
**Fig. 4** X-ray diffraction pattern of initial and heat-treated ITO particles

heating, the peaks of b and e disappeared. Figure 5 shows ratio of  $\text{SnO}_2$  in total mass  $\text{SnO}_2/(\text{SnO}_2+\text{In}_2\text{O}_3)$  for the initial and heat-treated ITO particles obtained by analysis using Rietveld refinement. The initial ratio of  $\text{SnO}_2$  was estimated to be 3.5 wt%, although Kojundo Chemical Laboratory Co., Ltd. used 5 wt%  $\text{SnO}_2$  for preparation of ITO particles used for the present experiment. A part of Sn atoms were probably incorporated into  $\text{In}_2\text{O}_3$  during heat treatment in the company. The ratio of  $\text{SnO}_2$  increased to 3.9 wt% by heat treatment at 800 °C. On the other hand, the ratio was markedly decreased by heat treatment at 1,000 °C. Moreover, no  $\text{SnO}_2$  was observed in the case of ITO particles heat treated at 1,300 °C. According to William J. Heward, the solubility of  $\text{SnO}_2$  in  $\text{In}_2\text{O}_3$  increases as temperature of heat treatment increases [27]. We believe that Sn atoms were completely incorporated into  $\text{In}_2\text{O}_3$  lattice sites by heating of ITO at 1,300 °C. We also believe that oxygen vacancies in ITO particles were simultaneously generated during heat treatment in vacuum through oxygen gas desorption. Figure 6 shows  $C_c$  of n-type Si sample (a) and p-type Si sample (b) which was serialized in descending order.

In the case of n-type Si sample, the highest  $C_c$  of 4.3 S/cm<sup>2</sup> was obtained for the n-type sample with 800 °C heated ITO.  $C_c$  was higher than 1.1 S/cm<sup>2</sup> for all n-type sample pieces formed with initial, 800 °C heated, and 1,000 °C heated ITO particles. 91 n-type sample pieces formed with 1,300 °C heated ITO particles also had  $C_c$  above 1.1 S/cm<sup>2</sup>. The average values of  $C_c$  in 100 pieces were 1.82, 1.83, 2.05, and 1.59 S/cm<sup>2</sup> for n-type samples formed with initial, 800 °C heated, 1,000 °C heated, and

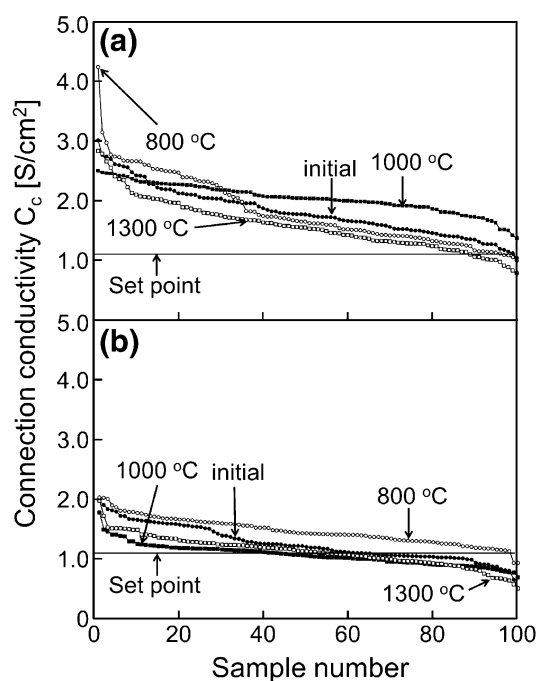
**Table 1** Angular positions and sources of XRD spectral peaks shown in Fig. 4

	$2\theta(^{\circ})$	Material
a	21.4	$\text{In}_2\text{O}_3$ (211)
b	26.5	$\text{SnO}_2$ (110)
c	30.5	$\text{In}_2\text{O}_3$ (222)
d	33.0	$\text{In}_2\text{O}_3$ (321)
e	33.8	$\text{SnO}_2$ (101)
f	35.4	$\text{In}_2\text{O}_3$ (400)
g	37.6	$\text{In}_2\text{O}_3$ (411)

**Fig. 5** Ratio of  $\text{SnO}_2$  in total mass  $\text{SnO}_2/(\text{SnO}_2 + \text{In}_2\text{O}_3)$  for initial and heat treated ITO particles

1,300 °C heated ITO particles, respectively. On the other hand, in the case of p-type Si samples, the  $C_c$  were lower than that of n-type Si samples. Numbers of sample pieces with  $C_c$  above 1.1  $\text{S}/\text{cm}^2$  were 70, 98, 49, and 60 for p-type samples formed with initial, 800 °C heated, 1,000 °C heated, and 1,300 °C heated ITO particles, respectively. The average values of  $C_c$  in 100 pieces were 1.24, 1.46, 1.06 and 1.11  $\text{S}/\text{cm}^2$  for p-type samples formed with initial, 800 °C heated, 1,000 °C heated, and 1,300 °C heated ITO particles, respectively. These results indicate that heating of ITO particles at 800 °C is useful. Figure 7 shows frequency probability as a function of  $C_c$  summarized with a  $C_c$  step of 0.1  $\text{S}/\text{cm}^2$  of p-type sample formed with 800 °C heated ITO particles shown in Fig. 6b. The probability distribution was fitted to the Gaussian distribution function as,

$$P(C_c) = \frac{\exp\left(-\frac{(C_c - a)^2}{2\sigma^2}\right)}{\int_0^{\infty} \exp\left(-\frac{(C_c - a)^2}{2\sigma^2}\right) dC_c} \quad (2)$$

**Fig. 6**  $C_c$  of n-type Si sample (a) and p-type Si sample (b) serialized in descending order

where  $a$ , and  $\sigma$  were  $C_c$  at the maximum frequency and standard deviation of  $C_c$ , respectively. The experimental and Gaussian curves were roughly fitted in the case of a, and  $\sigma$  were 1.47 and 0.228  $\text{S}/\text{cm}^2$ , respectively. Although ITO particles had different kinds of shape, we assumed that they had a sphere shape for simple discussion. When ITO particles with diameter of 20  $\mu\text{m}$  were uniformly dispersed in Cemedine at 6.2 wt%, about 290 ITO particles were distributed per area of  $0.6 \times 0.6 \text{ cm}^2$ . If ITO particles were randomly distributed on silicon pieces, a standard deviation of particles was proportional to the square root of number of particles. On an assumption of 290 ITO particles on  $0.6 \times 0.6 \text{ cm}^2$  Si piece gave the average  $C_c$  of 1.47  $\text{S}/\text{cm}^2$  shown above, one ITO particle has an effective conductivity of 0.0051  $\text{S}/\text{cm}^2$ . In this case, standard deviation of  $C_c$  is estimated to be about 0.087  $\text{S}/\text{cm}^2$ . This is much lower than experimental standard deviation of 0.228  $\text{S}/\text{cm}^2$ .

Figure 8 shows standard deviation of n-type and p-type samples. In the case of n-type Si sample, the standard deviation ranged from 0.59 to 0.24  $\text{S}/\text{cm}^2$ . In the case of p-type sample, the standard deviations were distributed around from 0.29 to 0.17  $\text{S}/\text{cm}^2$ . These results suggest that  $C_c$  was not seriously affected by the distribution of number of ITO particles under Si piece. Our microscope observation revealed that an average size of ITO particles was slightly decreased by heat treatment, and that the particles

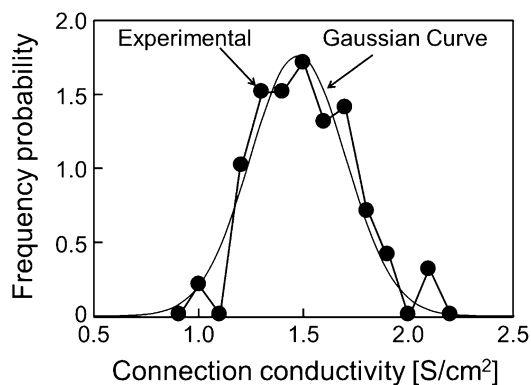


**Fig. 7** Frequency probability as a function of  $C_c$  summarized with a  $C_c$  step of  $0.1 \text{ S/cm}^2$  for the p-type Si sample formed with  $800^\circ\text{C}$  heated ITO particles. Gaussian curve fitting is also presented

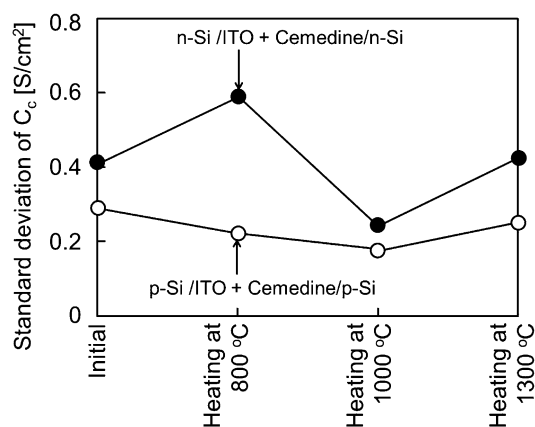


**Fig. 8** Standard deviation of  $C_c$  for the n-type and p-type Si samples

were uniformly dispersed in the adhesive with no serious agglomeration. There is a possibility of that the increases in  $C_c$  were induced by decrease in the size of ITO particles because superficial area of ITO particle per unit weight increased. On the other hand, distribution in  $C_c$  was also changed by heat treatment, as shown in Figs. 6, 7 and 8. This result indicates that all of ITO particles did not equally contact to the silicon surface. The contact probability between ITO and silicon can be changed by heat treatment.  $C_c$  is naturally governed by the ITO particle density per unit area, its average size, and contact probability.

Figure 9 shows J–V characteristics of n-type (a) and p-type Si samples (b) formed with  $800^\circ\text{C}$  heated ITO particles with  $C_c$  ranged from  $1.0$  to  $4.3 \text{ S/cm}^2$  and  $0.9$  to  $2.0 \text{ S/cm}^2$ , respectively. Both samples showed ohmic characteristics. ITO has many oxygen vacancies, which caused donor-like gap states in the upper half of the band gap [28–30]. Sn atoms in ITO had also donor states. Electron transfer between the silicon and ITO conduction

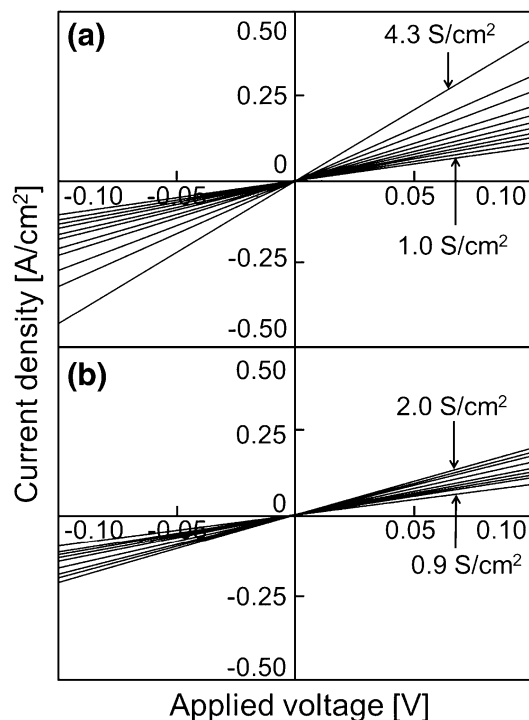


**Fig. 9** J–V characteristics of n-type (a) and p-type samples (b) formed with ITO particles heat treated at  $800^\circ\text{C}$

bands will easily occur via those energy states in spite of their band offset for the case of ITO particles and n-type Si contact. On the other hand, in the case of ITO particles and p-type Si contact, the higher band offset between the silicon valence and ITO conduction bands was overcome by recombination of holes in silicon and electrons in ITO with their wave function overlapping at the ITO/Si interface. We believe that the recombination probability slightly decreased  $C_c$  in the case of ITO particles and p-type Si contact with keeping ohmic characteristic compared with the case of ITO particles and n-type Si contact. High  $C_c$  and small distribution of  $C_c$  were simultaneously obtained for the n- and p-type sample with ITO particles heat treated at  $800^\circ\text{C}$ . These results indicate that there is possibility of fabrication of intermediate layer with high and narrow distribution of  $C_c$ . According to calculation shown in Fig. 2, present  $C_c$  above  $1.1 \text{ S/cm}^2$  achieves a low loss of  $E_{ff}$  lower than  $0.3 \%$  in the application of fabrication of multi junction solar cell with an intrinsic  $E_{ff}$  of  $30 \%$  and an open circuit voltage above  $1.9 \text{ V}$ .

## 5 Summary

We set the desired  $C_c$  as  $1.0 \text{ S/cm}^2$  according to calculation of solar cell characteristics. ITO particles with a diameter of  $20 \mu\text{m}$  were heated in vacuum by ranging heating

temperature from 800 to 1,300 °C. XRD measurement revealed that heating of ITO at 800 °C increases ratio of SnO<sub>2</sub>. On the other hand, the ratio of SnO<sub>2</sub> was decreased by heating of ITO above 800 °C. ITO particles at 6.2 wt% were mixed with commercial adhesive of Cemedine. They were coated over 4-inch n- or p-type 0.001 Ω cm Si substrates with 100, 0.6 × 0.6 cm<sup>2</sup> sized n- or p-type 0.001 Ω cm Si pieces were then placed on the adhesive. The Cemedine intermediate layers including ITO particles were hardened under a pressure at 4 × 10<sup>5</sup> Pa for 1 h. J–V characteristics were measured for each Si piece for n-type Si sample and p-type Si sample. In the case of n-type Si sample, sample formed with initial ITO, 800 °C heated ITO and 1,000 °C heated ITO showed high C<sub>c</sub> above 1.1 S/cm<sup>2</sup>. Especially, sample formed with 800 °C heated ITO showed high C<sub>c</sub> of 4.3 S/cm<sup>2</sup>. The standard deviation of sample with 800 °C heated ITO was 0.59 S/cm<sup>2</sup>. On the other hand, in the case of p-type Si sample, average C<sub>c</sub> increased from 1.24 to 1.46 S/cm<sup>2</sup> for the sample with 800 °C heated ITO. According to fitting of frequency probability of p-type Si sample formed with 800 °C heated ITO particles, distribution of ITO particles is not main reason for change in distribution of C<sub>c</sub>. The distribution of C<sub>c</sub> mainly resulted from contact efficiency of ITO particles to substrate. However, high and small distribution of C<sub>c</sub> was obtained for p-type sample. These results indicate that there is possibility of fabrication of intermediate layer with high C<sub>c</sub> with low standard deviation.

**Acknowledgments** This work was partly supported by Grant in Aid for Science Research C from the Ministry of Education, Culture, Sports, Science and Technology of Japan (Nos. 25420282 and 23560360), the New Energy and Industrial Technology Development Organization (NEDO).

## References

1. M. Tanaka, M. Taguchi, T. Matsuyama, T. Sawada, S. Tsuda, S. Nakano, H. Hanafusa, Y. Kuwano, *Jpn. J. Appl. Phys.* **31**, 3518 (1992)
2. J. Zhao, A. Wang, M.A. Green, F. Ferrazza, *Appl. Phys. Lett.* **73**, 1991 (1998)
3. O. Schultz, S.W. Glunz, G.P. Willeke, *Prog. Photovolt. Res. Appl.* **12**, 553 (2004)
4. A.V. Shah, H. Schade, M. Vanecek, J. Meier, E. Vallat-Sauvain, N. Wyrsh, U. Kroll, C. Droz, J. Bailat, *Prog. Photovolt. Res. Appl.* **12**, 113 (2004)
5. S. Chhajed, M.F. Schubert, J.K. Kim, E.F. Schubert, *Appl. Phys. Lett.* **93**, 251108 (2008)
6. H. Sugiura, C. Amano, A. Yamamoto, M. Yamaguchi, *Jpn. J. Appl. Phys.* **27**, 269 (1988)
7. J.M. Olson, S.R. Kurtz, A.E. Kibbler, P. Faine, *Appl. Phys. Lett.* **56**, 623 (1990)
8. T. Takamoto, E. Ikeda, H. Kurita, M. Ohmori, M. Yamaguchi, M.J. Yang, *Jpn. J. Appl. Phys.* **36**, 6215 (1997)
9. M. Yamaguchi, *Sol. Energy Mater. Sol. Cells.* **75**, 261 (2003)
10. M. Yamaguchi, T. Takamoto, K. Araki, N. Ekings-Daukes, *Sol. Energy* **79**, 78 (2005)
11. M. Yamaguchi, T. Takamoto, K. Araki, *Sol. Energy Mater. Sol. Cells.* **90**, 3068 (2006)
12. M. Yamaguchi, K. Nishimura, T. Sasaki, H. Suzuki, K. Arafune, N. Kojima, Y. Oshita, Y. Okada, A. Yamamoto, T. Takamoto, K. Araki, *Sol. Energy.* **82**, 173 (2008)
13. E.A. Katz, J.M. Gordon, D. Feuermann, *Prog. Photovolt. Res. Appl.* **14**, 297 (2006)
14. F. Meillaud, A. Shah, C. Droz, E. Vallat-Sauvain, C. Miazza, *Sol. Energy Mater. Sol. Cells* **90**, 2952 (2006)
15. R.R. King, D.C. Law, K.M. Edmondson, C.M. Fetzer, G.S. Kinsey, H. Yoon, R.A. Sherif, N.H. Karam, *Appl. Phys. Lett.* **90**, 183516 (2007)
16. D.J. Friedman, *Curr. Opin. Solid State Mater. Sci.* **14**, 131 (2010)
17. A. Hadipour, B.D. Boer, P.W.M. Blom, *Adv. Funct. Mater.* **18**, 169 (2008)
18. T. Saga, *NPG Asia Mater.* **2**, 96 (2010)
19. T. Sameshima, J. Takenezawa, M. Hasumi, T. Koida, T. Kaneko, M. Karasawa, M. Kondo, *Jpn. J. Appl. Phys.* **50**, 052301 (2011)
20. T. Karasawa, Y. Miyata, *Thin Solid Films* **223**, 135 (1993)
21. S. Yoshidomi, M. Hasumi, T. Sameshima, K. Makita, K. Matsubara, M. Kondo, in *Proceedings of 6th Thin Film Materials & Devices Meeting 130222027-1* (2012)
22. J. Takenezawa, C. Akiyama, M. Hasumi, T. Sameshima, *International Symposium on Innovative Solar Cells 2012*, p 10 (Tokyo, 2012)
23. E. Karatepe, M. Boztepe, M. Colak, *Sol. Energy* **81**, 977 (2007)
24. K. Ishibashi, Y. Kimura, M. Niwano, *J. Appl. Phys.* **103**, 094507 (2008)
25. J.H. Lee, S. Cho, A. Roy, H. Jung, A.J. Heeger, *Appl. Phys. Lett.* **96**, 163303 (2010)
26. A.B. Or, J. Appelbaum, *Prog. Photovolt.* **21**, 713 (2013)
27. W.J. Heward, D.J. Swenson, *J. Mater. Sci.* **42**, 7135 (2007)
28. O.N. Mryasov, A.J. Freeman, *Phys. Rev. B.* **64**, 233111 (2001)
29. M. Batzill, U. Diebold, *Prog. Surf. Sci.* **79**, 47 (2005)
30. A. Walsh, C.R.A. Catlow, *J. Mater. Chem.* **20**, 10438 (2010)